Structure of a non-bulk termination of the clean $Pt_3Sn(111)$ surface: a study by low-energy electron diffraction and X-ray photoelectron diffraction

1993 J. Phys.: Condens. Matter 5 L207

(http://iopscience.iop.org/0953-8984/5/14/003)

J. Phys.: Condens. Matter 5 (1993) L207–L212. Printed in the UK

LETTER TO THE EDITOR

Structure of a non-bulk termination of the clean $Pt_3Sn(111)$ surface: a study by low-energy electron diffraction and x-ray photoelectron diffraction

A Atrei†, U Bardi†, M Torrini†, E Zanazzi†, G Rovida†, H Kasamura‡ and M Kudo‡

† Dipartimento di Chimica, Università di Firenze, 50121 Firenze, Italy
‡ Material Science and Technology Foundation, 3-11-1 Kamisoshigaya, Setagaya-Ku, Tokyo 157, Japan

Received 11 January 1993

Abstract. A non-bulk termination with a $(\sqrt{3} \times \sqrt{3})R30°$ periodicity was observed on the clean $Pt_3Sn(111)$ surface. X-ray photoelectron diffraction and low-energy electron diffraction showed that this phase is a mixed Sn–Pt topmost layer which is enriched in tin with respect to the bulk composition. The data also indicate that the subsurface region is depleted in tin. The structure of the $(\sqrt{3} \times \sqrt{3})R30°$ phase is the same as that of the phase observed in the case of tin deposited on the clean Pt(111) surface.

The Pt–Sn system has been extensively investigated by surface sensitive techniques in view of the interest in Pt–Sn alloys as catalysts for hydrocarbon conversion and as electrocatalysts for the direct oxidation of methanol in fuel cells [1–3]. Recently, reconstructed surface phases of periodicity other than expected for bulk truncation have been reported for the $Pt_3Sn(100)$ and $Pt_3Sn(110)$ surfaces [4–6]. In the present work we report the observation of a surface reconstruction, also for the case of the clean $Pt_3Sn(111)$ surface. This reconstruction has a $(\sqrt{3} \times \sqrt{3})R30°$ periodicity. We show that the formation of the $(\sqrt{3} \times \sqrt{3})R30°$ phase is triggered by a depletion of tin in the subsurface layers and that this phase is a mixed Sn–Pt single atomic layer over an Sn-depleted subsurface region. This structure is the same as that observed for Sn deposited on Pt(111) [7–9]. To our knowledge, this is the first case where a non-bulk termination of the surface of a binary alloy has been examined by quantitative surface crystallographic techniques.

The experiments were performed in a vacuum chamber capable of base pressures in the 10^{-8} Pa range. The chamber was equipped with a hemispherical electron analyser and four-grid optics for low-energy electron diffraction (LEED). The $Pt_3Sn(111)$ single-crystal sample was mounted on a manipulator that permitted polar and azimuthal rotation, and annealing up to approximately 1000 K. Non-monochromatized Al $K\alpha$ was used as radiation source for x-ray photoelectron spectroscopy (XPS) and x-ray photoelectron diffraction (XPD) measurements. The angle between the x-ray source and the analyser was 55° and the semicone angle of acceptance of the analyser was 2.5°. XPD curves were collected by monitoring the intensity of the Pt $4f_{7/2}$ (1410 eV kinetic energy), Pt $4p_{3/2}$ (960 eV) and Sn

0953-8984/93/140207+06$07.50

$3d_{5/2}$ (994 eV) photoemission peaks as a function of the angle. The background was estimated by measuring the intensity of the XPS signal at a kinetic energy 5–10 eV higher than the value corresponding to the photoemission peak. The anisotropy in the XPD curves is defined here as $(I_{max} - I_{min})/I_{max}$. LEED intensity versus potential (I–V) curves were collected by means of a video system in a range of primary electron energies from 30 to 150 eV.

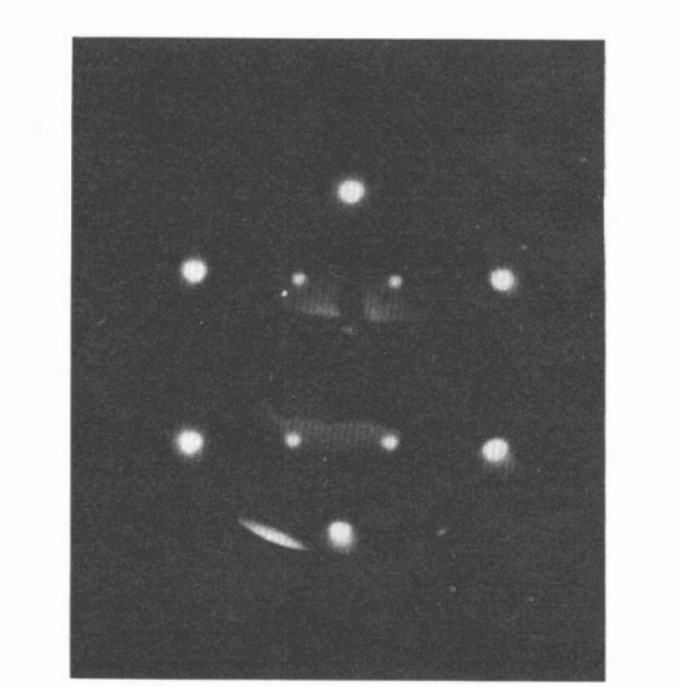

Figure 1. LEED pattern showing the $(\sqrt{3} \times \sqrt{3})R30°$ superstructure on the $Pt_3Sn(111)$ surface. The primary energy is 57 eV.

The initial contamination of the $Pt_3Sn(111)$ surface was removed by cycles of Ar^+ sputtering at 1 keV at room temperature and successive annealing up to 1000 K for several minutes. After cleaning, successive cycles of sputtering and annealing in the same conditions produced a reproducible Pt/Sn XPS signal ratio and a sharp LEED pattern. The unit mesh observed in these conditions corresponds to the ideal truncation of the bulk Pt_3Sn alloy along the (111) plane. This pattern can be described as a p(2×2), indexing the diffraction spots with respect to the periodicity of the Pt(111) surface [5, 6]. A different pattern was observed when the $Pt_3Sn(111)$ surface was sputtered with 3 keV Ar^+ ions while the sample was held at 600 K. This pattern (figure 1) corresponds to a $(\sqrt{3} \times \sqrt{3})R30°$ superstructure (also indexed with respect to the Pt(111) periodicity). In these conditions the pattern is sharp and does not show any fractional-order spots corresponding to the p(2×2) phase. Extended annealing at 1000 K caused the progressive disappearance of the $(\sqrt{3} \times \sqrt{3})R30°$ phase, gradually replaced by the p(2×2) phase.

Experimental and calculated XPD azimuthal curves for the bulk truncation p(2×2) phase are shown in figure 2. The threefold symmetry of this surface is reproduced

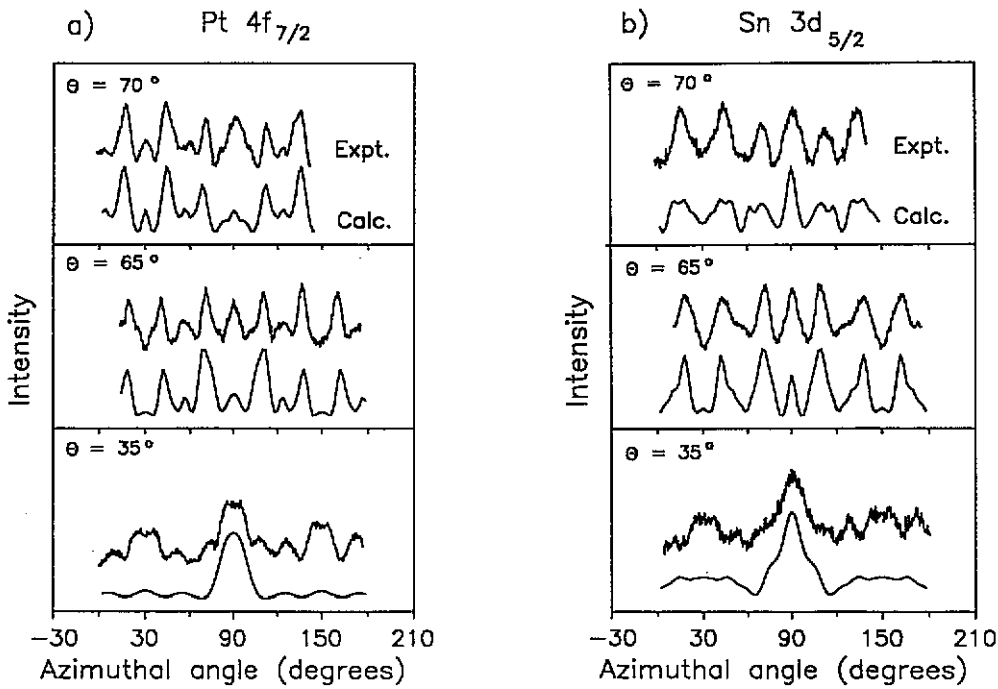

Figure 2. Experimental and calculated XPD azimuthal curves for the p(2×2) phase of $Pt_3Sn(111)$. The polar angle of emission Θ is measured with respect to the normal to the surface: (*a*) Pt $4f_{7/2}$, (*b*) Sn $3d_{5/2}$.

in the experimental XPD plots. For the calculation, we used the single-scattering cluster–plane wave model (SSC–PW) [10, 11], using phase shifts derived from muffin tin potentials for Pt and Sn. The structural model used in the calculation was derived from our previous LEED structural analysis of this surface [6], which corresponds to the ideal truncation structure. For this model, the agreement between theory and experiment is fairly good (figure 2), with major discrepancies only for the data at Θ = 35°. The most intense peak in the data at this angle is due to forward scattering enhancement along the close packed ⟨110⟩ atomic rows of the FCC Pt_3Sn lattice. In this case, the SSC–PW calculation overestimates the relative intensity of the forward scattering peaks [11]. The XPD calculation was found to be scarcely sensitive to variations in the structural parameters of the topmost surface plane (Sn or Pt buckling, interplane distance) that could instead be optimized in the LEED analysis [6].

Azimuthal XPD curves for the $(\sqrt{3} \times \sqrt{3})R30°$ phase are reported in figure 3, compared with those for the p(2×2) phase at the same polar angles. The shapes and positions of the peaks in these curves are the same within the experimental incertitude. However the overall anisotropy of the Sn 3d curve measured in comparison to the total Sn signal is significantly lower for the $(\sqrt{3} \times \sqrt{3})R30°$ phase. In contrast, the anisotropy for the Pt 4f signal remains nearly the same. We can rule out the possibility that this effect is caused by the different escaping depth of the Pt $4f_{7/2}$ and Sn $3d_{3/2}$ photoelectrons, since virtually identical results were obtained monitoring the Pt $4p_{3/2}$ peak that has a kinetic energy close to that of Sn $3d_{5/2}$.

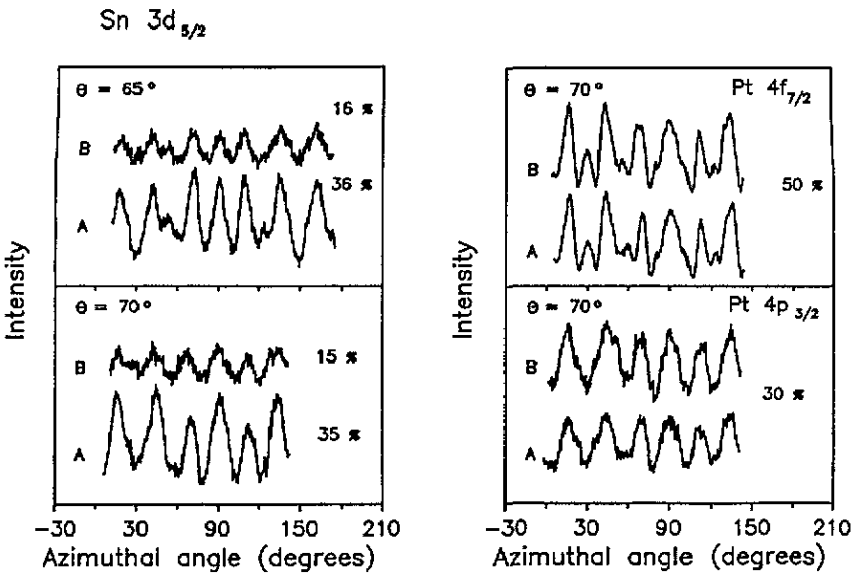

Figure 3. Azimuthal XPD curves for the p(2×2) (curves A) and $(\sqrt{3} \times \sqrt{3})$R30° (curves B) structures. On the left side are XPD curves for the Sn $3d_{5/2}$ photoemission peak at $\Theta = 65°$ and $\Theta = 70°$. On the right side are azimuthal XPD curves for the Pt $4f_{7/2}$ and Pt $4p_{3/2}$ photoemission peaks at $\Theta = 70°$. For all the curves the reported values of the anisotropy are defined as $(I_{max} - I_{min})/(I_{max})\%$, where I_{max} and I_{min} are the maximum and minimum intensities in the XPD curves.

A depletion of tin in the subsurface region of the $(\sqrt{3} \times \sqrt{3})$R30° phase could explain the lower amplitude of the XPD oscillations of the Sn 3d signal. Since diffraction effects in the range of energies used in the present work are dominated by forward scattering enhancement [11], the signal from tin atoms in the topmost layer is expected to oscillate weakly, unlike that from tin in the subsurface. The low anisotropy of the XPD curves indicate therefore a low tin concentration in the subsurface region. XPS measurements of the Sn/Pt signal area ratio as a function of the take-off angle confirm the depletion of tin in the subsurface layers. Another indication of strong Sn depletion in the bulk is the disappearance of the fractional-order LEED beams corresponding to the p(2×2) when the $(\sqrt{3} \times \sqrt{3})$R30° phase is present. The similarity of the XPD curves also indicate that the subsurface Sn atoms should be located in the same substitutional sites for both the reconstructed and the unreconstructed surface.

Information about the structure of the reconstructed topmost layer can be obtained by LEED. Data for this purpose can be obtained from the comparison of the LEED I–V curves for the $(\sqrt{3} \times \sqrt{3})$R30° phase of the $Pt_3Sn(111)$ alloy with those for the phase with the same surface unit mesh that is obtained depositing Sn on Pt(111). In a recent work [7] we performed a complete LEED structural analysis of the Pt(111) $(\sqrt{3} \times \sqrt{3})$R30°–Sn surface, showing that this phase is a mixed Pt–Sn overlayer in agreement with the conclusions of previous studies [8, 9]. In figure 4 we show a comparison of some LEED I–V curves for the $(\sqrt{3} \times \sqrt{3})$R30° reconstructed $Pt_3Sn(111)$ alloy and for the Pt(111) $(\sqrt{3} \times \sqrt{3})$R30°–Sn phase. The similarity of the two sets of experimental curves shows that both systems have the same structure,

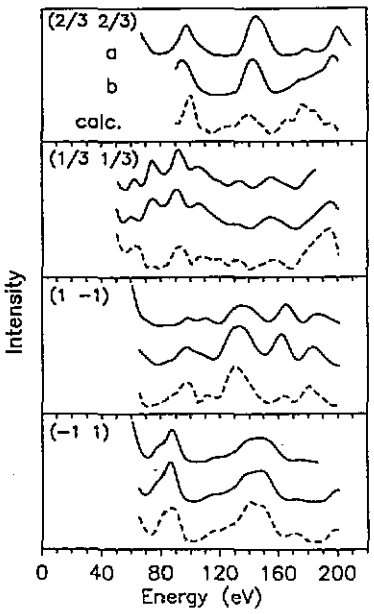

Figure 4. Comparison between the experiment LEED I–V curves for the $(\sqrt{3}\times\sqrt{3})$R30° phase of the $Pt_3Sn(111)$ surface (curves a) and for the surface alloy of the same $(\sqrt{3}\times\sqrt{3})$R30° periodicity formed by deposition of Sn on the Pt(111) surface (curves b). The calculated LEED I–V (broken) curves correspond to the optimized model for the Pt(111)$(\sqrt{3}\times\sqrt{3})$R30° surface alloy, shown in figure 5.

and is a further element indicating a strong tin depletion in the subsurface layers of the reconstructed Pt_3Sn alloy. In figure 4 we also report the calculated I–V curves that correspond to the optimized structural model for the Pt(111) $(\sqrt{3}\times\sqrt{3})$R30°–Sn phase. A full account of the experimental and theoretical procedure for the LEED structural analysis of the Pt/Sn system is reported elsewhere [6, 7]. The structural model is shown in figure 5 and consists of a topmost plane where Sn atoms substitute Pt atoms in an orderly way according to the $(\sqrt{3}\times\sqrt{3})$R30° periodicity, while the underlying layers of the allow are assumed to contain no tin. The optimization of the structural parameters in the LEED analysis leads to a slight upward buckling (~0.2 Å) of the Sn atoms in the overlayer. The $(\sqrt{3}\times\sqrt{3})$R30° model can be compared with the p(2×2) bulk truncation termination model (also shown in figure 5). The Sn fraction in the topmost layer for these models is, respectively, 1/3 and 1/4 of a monolayer.

The subsurface tin depletion of the $Pt_3Sn(111)$ $(\sqrt{3}\times\sqrt{3})$R30° phase may be the result of a mechanism involving preferential sputtering of Sn from the surface region and diffusion of Sn onto the surface from the bulk. This process may lead to a steady state condition where the subsurface layers are depleted in tin, even though the concentration of tin in the topmost layer is higher than in the bulk. The depletion of tin in the subsurface appears to be the critical factor that stabilizes the $(\sqrt{3}\times\sqrt{3})$R30° termination. Indeed the $(\sqrt{3}\times\sqrt{3})$R30° phase obtained by deposition of Sn on Pt(111) is stable upon annealing [7, 8], whereas in $Pt_3Sn(111)$ the high-temperature diffusion of tin from the bulk eventually restores the bulk truncation structure.

The formation of the $(\sqrt{3}\times\sqrt{3})$R30° phase on $Pt_3Sn(111)$ may be qualitatively

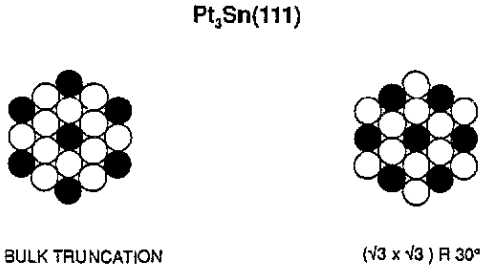

Figure 5. Structural models for the p(2×2) bulk termination and the $(\sqrt{3} \times \sqrt{3})$R30° reconstruction of the $Pt_3Sn(111)$ alloy.

interpreted considering that the ordered FCC Pt_3Sn alloy has a highly negative enthalpy of formation [12, 13], that may be attributed in part to the localized Pt–Sn nearest-neighbour interaction. In the $(\sqrt{3}\times\sqrt{3})$R30° phase, Sn atoms are surrounded by Pt atoms only, and this structure maximizes the number of Sn atoms that do not have other Sn neighbours in the same plane. However, when the $(\sqrt{3} \times \sqrt{3})$R30° phase exists on top of an unreconstructed, ordered $Pt_3Sn(111)$ plane, then a number of Sn–Sn nearest-neighbour pair must exist between atoms of the first and the second surface layers. In contrast, in the p(2×2) bulk termination such pairs do not exist. This factor may stabilize the $(\sqrt{3} \times \sqrt{3})$R30° phase when the subsurface layers of $Pt_3Sn(111)$ are depleted in tin.

The combination of XPD and LEED leads to the determination of the structure of the $(\sqrt{3} \times \sqrt{3})$R30° reconstruction of the $Pt_3Sn(111)$ surface. The XPD results show that tin atoms in the subsurface layers occupy the same substitutional sites as in the unreconstructed surface; however the subsurface region is strongly depleted in tin. The LEED results show that the structure of the $(\sqrt{3} \times \sqrt{3})$R30° overlayer on the $Pt_3Sn(111)$ surface is the same as that of the layer obtained depositing Sn on Pt(111) and indicate that it consists of a mixed Sn–Pt topmost layer.

This work was supported by the Consiglio Nazionale delle Ricerche (Italy) under the progetto finalizzato 'Chimica Fine II' and by the Foundation for Promotion of Material Science and Technology (Japan).

References

[1] Bouwman R, Toneman L H and Holsher A A 1973 *Surf. Sci.* **35** 8
[2] Hoflund G B, Asbury D A, Kirszensztein P and Laitinen H A 1985 *Surf. Sci.* L583
[3] Asbury D A and Hoflund G B 1988 *Surf. Sci.* 552
[4] Haner A N, Ross P N and Bardi U 1991 *Catal. Lett.* **8** 1
[5] Haner A N, Ross P N and Bardi U 1991 *Surf. Sci.* **249** 15
[6] Atrei A, Bardi U, Rovida G, Torrini M, Zanazzi E and Ross P N 1992 *Phys. Rev.* B **46** 1649
[7] Atrei A, Bardi U, Wu J X, Rovida G and Torrini M 1993 *Surf. Sci.* submitted
[8] Paffet M T and Windham R G 1989 *Surf. Sci.* **208** 34
[9] Overbury S H, Mullin D R, Paffet M T and Koel B E 1991 *Surf. Sci.* **254** 45
[10] Fadley C S 1991 *Synchrotron Radiation Research: Advances in Surface Science* ed R Z Bachrach (New York: Plenum)
[11] Kaduwela A, Friedman D J and Fadley C S 1991 *J. Electron Spectrosc. Relat. Phenom.* **57** 223
[12] Van Santen R A and Sachtler W M H 1974 *J. Catal.* **33** 202
[13] Ferro R, Capelli R, Borsese A and Delfino S 1973 *Atti Accad. Naz. Lince Cl. Sci. Fic. Mater. Nat.* **54** 634